Water Resources and Industry 18 (2017) 17–32

Contents lists available at ScienceDirect

Water Resources and Industry

journal homepage: www.elsevier.com/locate/wri

# Electrical energy per order determination for the removal pollutant from industrial wastewater using UV/$Fe^{2+}$/$H_2O_2$ process: Optimization by response surface methodology

P. Asaithambi[a,b,*], Esayas Alemayehu[c], Baharak Sajjadi[a], Abdul Raman Abdul Aziz[a,**]

[a] Department of Chemical Engineering, Faculty of Engineering, University of Malaya, 50603, Malaysia
[b] School of Chemical Engineering, Jimma Institute of Technology, Jimma University, Jimma, Ethiopia
[c] School of Civil and Environmental Engineering, Jimma Institute of Technology, Jimma University, Jimma, Ethiopia

ARTICLE INFO

*Keywords:*
UV/$Fe^{2+}$/$H_2O_2$ process
Distillery
Color and COD removal
Electrical energy per order
RSM

ABSTRACT

Comparison of UV, $H_2O_2$, $Fe^{2+}$, UV/$H_2O_2$, UV/$Fe^{2+}$, $Fe^{2+}$/$H_2O_2$ and UV/$Fe^{2+}$/$H_2O_2$ processes for the removal of percentage color, COD and electrical energy per order from the effluent distillery industry. The results showed that, UV/$Fe^{2+}$/$H_2O_2$ process yield higher percentage color and COD removal with low electrical energy per order than UV, UV/$H_2O_2$, UV/$Fe^{2+}$ process. To obtain the UV/$Fe^{2+}$/$H_2O_2$ process performance by operating various parameters on the percentage color and COD removal using response surface methodology. A Regression quadratic model describing the percentage color and COD removal efficiency of UV/$Fe^{2+}$/$H_2O_2$ process were developed and validate by analysis of variance. Experimental results showed that, UV/$Fe^{2+}$/$H_2O_2$ process can effectively reduced 96.50% of color and 84.40% of COD removal of the distillery industry wastewater under the optimum conditions such as $Fe^{2+}$–1.50 mM, $H_2O_2$–200 mM, COD–1500 ppm and pH–3.2, respectively. Result concluded that, UV/$Fe^{2+}$/$H_2O_2$ process can be used effectively for the treatment of real industrial effluent.

## 1. Introduction

Important current environmental problem is to treat the industrial effluent and this is a very difficult task due to the variety of industrial effluent from various industries such as textile [1], leather [2], pharmaceutical [3], pulp and paper [4], distillery [5,6], petroleum [7], agro –industrial [8], heavy metal [9], etc. Considering the distillery industry effluent is the most important one, due to the generation huge amount wastewater various stages. The effluent containing persistent organic compound, dark brown color, high Chemical Oxygen Demand (COD), Biological Oxygen Demand (BOD) and Total Dissolved Solids (TDS), Total Suspended Solids (TSD) and low pH, etc. If it is not properly treated the industrial effluent, before discharge into the water bodies. The effluent can not only cause environmental deterioration but also adversely affect the human health [10]. In order to, avoid deterioration of water resources and reuse treated industrial wastewater from an effluent treatment technique, taking also into consideration that organic and inorganic compounds in effluents are insufficiently removed by conventional physical, chemical and biological process. Advanced oxidation processes (AOPs) are being studied as an alternative option to the traditional methods [11]. AOPs are effective methods for removing organic and inorganic pollutants from an industrial wastewater because; it can destroy hazardous contaminants, and not simply transfer them from one phase to another phase as do conventional treatment techniques [12–14]. The main advantage of AOPs

* Corresponding author at: Department of Chemical Engineering, Faculty of Engineering, University of Malaya, 50603, Malaysia.
** Corresponding author.
*E-mail addresses:* drasaithambi2014@gmail.com (P. Asaithambi), azizraman@um.edu.my (A.R.A. Aziz).

http://dx.doi.org/10.1016/j.wri.2017.06.002
Received 13 June 2016; Received in revised form 18 February 2017; Accepted 7 June 2017

comparing with biological, physical and chemical process was destructive nature that causes mineralization of organic contaminants in wastewater and it was as low-or even non-waste generation technologies, and produce short-lived chemical species with a great power of oxidation (˙OH). Hydroxyl radicals (˙OH) are the main oxidizing species produced by AOPs, because of its non-selectivity and high reactivity. Many researchers have been taken efforts to eliminate the pollutant from various industrial effluent using AOPs like catalytic wet oxidation [15], ozonation and Fenton's oxidation [16], Fenton process [17], photo-Fenton process [18–20] and combined sono–photo-Fenton process [21]. In all these processes, Fenton and photo-Fenton process appears to be most promising method considering overall removal efficiency of the process based on high reaction yield, offer a cost effective source of $HO^{\bullet}$ and it is easy to operate and maintain [21,22]. Hideyuki Katsumata et al. studied the photo-Fenton degradation of alachlor in the presence of citrate solution and reported that, this method can be applied to wastewater treatment as a new developing methodology for reducing the pollutant [23,24]. Lucas and Peres, investigated the decolorization of azo dye Reactive Black 5 using Fenton and photo-Fenton process and found that the complete decolorization of dye in shorter reaction time [25]. Elmorsi et al., studied the decolorization of Mordant red 73 azo dye using photo-Fenton process and found that this method was promising techniques for the degradation of MR73 dye [26]. Yamal-Turbay et al., studied and reported, that the photo-Fenton treatment has effective process for removing the tetracycline from water solutions [27]. Affam et al. reported that, the UV-Fenton process is effective treatment for pesticide wastewater and to meet the Malaysian industrial effluent discharge standard [28]. From the literature review, many investigations have been used for the treatment of industrial effluent using the methods of UV treatment, UV/$H_2O_2$, $Fe^{2+}$/$H_2O_2$ and UV/$Fe^{2+}$/$H_2O_2$ process [24,25,29–31]. All the earlier cited works carried out for the pollutant removal using synthetic solution and only few works has been studied for the pollutant removal using real effluent. The most of the research work has focus on treatment efficiency based on decolorization and degradation. In photo based AOPs, the electrical energy per order having important parameter due to operating costs and economical point of view of the process. So in this research work, we are focus on the removal of pollutant (in terms of % color and COD removal efficiency) and also determination of electrical energy per order by UV/$Fe^{2+}$/$H_2O_2$ process from the distillery industrial effluent using RSM.

### 1.1. Response surface methodology (RSM)

In the photo-Fenton system, many factors such as $Fe^{2+}$ and $H_2O_2$ concentration, effluent COD concentration and pH were influence of UV/$Fe^{2+}$/$H_2O_2$ process. The hybrid process efficiency may be increased by optimization of these factors using RSM. In conventional multifactor experiments, optimization is usually carried out by varying a single factor while keeping all the other factors fixed at specific set of conditions [32–34]. This method was time consuming and incapable of effective optimization. Recently, Response Surface Methodology (RSM) has been employed to optimize and understand the performance of complex systems [35,36]. By application of RSM it was possible to evaluate the interactions of possible influencing factors on treatment efficiency with a limited number of planned experiments.

RSM is a type of mathematical and statistical technique used for experimental design, building models, assessing relative significance of several independent variables synergism and determining the optimal conditions for desirable response [37]. In this study, the main objective is to optimize the response surface that is influenced by process parameters. RSM also quantifies the relationship between controllable input parameters and obtained response surfaces [38]. Process optimization by RSM was faster for gathering experimental research results than the rather conventional, time consuming one factor- at-a-time approach [39–41]. In RSM, the two most common designs extensively used are Box-Behnken Design (BBD) and Central Composite Design (CCD). The Box-Behnken designs are a collection of three-level designs that have various geometric constructions. The CCD consist of (a) factorial points, which are a $2^k$ design or $2^{k-f}$ fractional factorial design of at least resolution V, (b) star or axial points, which have each factor in turn set to its high and low levels and the other factors at central level, and (c) center points, which have all factors set to their central level. In the present study, CCD was selected as standard RSM for optimizing the operating parameters ($Fe^{2+}$ concentration, $H_2O_2$ concentration, effluent COD concentration and effluent initial pH). The CCD was selected in this study because of its efficiency with respect to number of runs required for fitting a second order response surface model [42]. In addition, CCD was ideal for sequential experimentation and allows a reasonable amount of information for testing lack of fit while not involving an unusually large number of design points [43] to provide high quality predictions over the entire design space in comparison with Box-Behnken Design [44].

The general structure of the second-order mathematical model, with interactions according to the depended variable ($Y_i$) in the response surface analysis, is:

$$Y_i = b_0 + \sum_{i=1}^{n} b_i x_i + \sum_{i=1}^{n} b_{ii} x_i^2 + \sum_{j=i+1}^{n} b_{ij} x_i x_j \quad (1)$$

where, Yi is the value of the color and COD removal, b0 is the constant coefficient, bi(i = 1,2,3 and 4) is the linear coefficients, bii (i = 1,2,3 and 4) is the quadratic coefficients, bij (i = 1,2,3 and 4; j = 1,2,3 and 4) is the interaction coefficients and *xi*, *xj* are the coded values of the factors [44]. The Design Expert (Version 9.0.6.2) was used for the data processing. Experimental data were fitted to a second-order polynomial equation, and regression coefficients were obtained. The analysis of variance (ANOVA) was performed to justify the significance and adequacy of developed regression model. The response surface models adequacy were evaluated by calculation of determination coefficient (R2) and testing it for the lack of fit.

The objective of this study is: (1). The comparison of UV, $H_2O_2$, $Fe^{2+}$, UV/$H_2O_2$, UV/$Fe^{2+}$, $Fe^{2+}$/$H_2O_2$ and UV/$Fe^{2+}$/$H_2O_2$ process in terms of color and COD removal efficiency with electrical energy per order and select the best one. (2). To study and

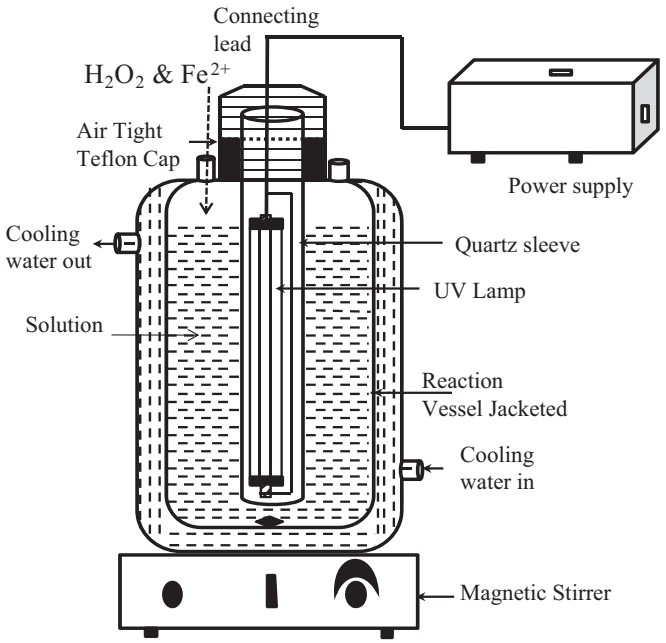


**Fig. 1.** Experimental setup of UV/$Fe^{2+}$/$H_2O_2$ process.

optimize operating factors such as $Fe^{2+}$ concentration (0.5–2.55 mM), $H_2O_2$ concentration (50–250 mM), effluent COD concentration (1000–5000 ppm) and effluent pH 2–4) on the percentage color, COD removal and determination of electrical energy per order from distillery industry wastewater by applying the CCD under RSM and (3). To verify the fitted model and determine the optimum experimental conditions for the removal of color and COD from distillery industrial effluent using UV/$Fe^{2+}$/$H_2O_2$.

## 2. Material and methods

### 2.1. Material

The distillery industrial effluent was used in this study and collected from nearby industry. The main characteristics of the effluent are: Chemical Oxygen Demand (COD): 80,000–90,000 mg $L^{-1}$, Biological Oxygen Demand (BOD): 7000–8000 mg $L^{-1}$, pH: 4.1-4.3, Total Suspended Solids (TSS): 15.44 $gL^{-1}$, Total Dissolved Solids (TDS): 5550–5750 mg $L^{-1}$, Color – dark brown, odor – burnt sugar. The following chemicals used in the present study: Hydrogen per oxide (50% w/w), Ferrous sulfate heptahydrate ($FeSO_4{\cdot}7H_2O$), and $H_2SO_4$, NaOH to adjust the pH value. All the chemicals were analytical grade and purchased from Merck Company. Double distilled water is used to prepare the solutions in all experiments.

### 2.2. Methods

The experimental set-up of the reactor employed for photochemical treatment of the industrial effluent is shown in Fig. 1. The photochemical reactor made of borosilicate glass with net capacity of 1000 mL. The reactor is surrounded with a water-cooling jacket to remove the heat produced by UV lamp and to maintain a constant temperature and also photochemical reactor outside covered with an aluminum foil to avoid any light leakage to the outside. top of photochemical reactor have an inlet and outlet port to feeding catalyst and withdraw the sample. The volume of effluent was used 750 mL and pH of solution was adjusted using proper NaOH and $H_2SO4$ solution. The photochemical reactor was placed on a magnetic stirrer to maintain a uniform effluent concentration. The source of UV irradiation was a 16 W low-pressure mercury vapor lamp with maximum emission at 254 nm placed in a quartz tube. The UV lamp was immersed in the effluent and to be treated. During the photochemical reaction, different time intervals of samples were collected from sampling port and quenched with $Na_2SO_3$ to arrest the solution, then filtrate using a filter paper and immediately to find out the color removal (Spectroquant Pharo® 300) and COD removal (Spectroquant® TR320).

### 2.3. Analysis

#### 2.3.1. Percentage color and COD removal

The removal color and COD (%) of sample was calculated using the below equation

$$\text{Color removal, } (\%) = 1 - \frac{Abs_t}{Abs_0} \times 100 \tag{2}$$

where,

$Abs_0$ and $Abs_t$ are the absorbance of initial and at any time $t$ samples for corresponding wavelength $\lambda_{max}$

$$\text{COD removal, } (\%) = 1 - \frac{COD_t}{COD_0} \times 100 \tag{3}$$

where,

$COD_0$ and $COD_t$ (ppm) are the Chemical Oxygen Demand (COD) at time $t = 0$ (initial) and at $t$ (reaction time) respectively.

*2.3.2. Electrical energy per order evaluation*

Energy efficiency of UV based AOPs is usually quoted in terms of electrical energy per order. The major fraction of operating cost in photochemical process is mainly associated with electrical energy per order and it can be defined as the number of kWhr (kilo Watt hour) of electrical energy required to reduce the concentration of a pollutant by 1st order of magnitude in 1 $m^3$ of contaminated water [29]. The electrical energy per order can be calculated by using the Eq. (4).

$$\text{Electrical energy per order} = \frac{P_{el} \times t \times 1000}{V \times 60 \times log\left(\frac{COD_i}{COD_t}\right)}, \text{(kWhr/m3order1)} \tag{4}$$

where,

$P_{el}$ is the rated power (in kW), $t$ is the irradiation time (in min), $V$ is the volume of effluent taken (in litre), $COD_i$ and $COD_t$is the COD concentration (in ppm) at initial and final.

The COD removal of industrial effluent was investigated using the pseudo-first-order kinetic model, as shown in Eq. (5).

$$log\left(\frac{COD_i}{COD_t}\right) = kt \tag{5}$$

where,

$k$ is the pseudo first order rate constant for the decay of the effluent COD concentration ($min^{-1}$)

Combining the above Eqs. (4) and (5) simply gives an equation for the electrical energy determination in the form

$$\text{Electrical enegy per order} = \frac{38.4 * P_{el}}{V * k} \tag{6}$$

## 3. Results and discussions

### 3.1. Comparison of UV, $H_2O_2$, $Fe^{2+}$, UV/$H_2O_2$, UV/$Fe^{2+}$, $Fe^{2+}$/$H_2O_2$ and UV/$Fe^{2+}$/$H_2O_2$ processes

In the first part of the study is UV, $H_2O_2$, $Fe^{2+}$, UV/$H_2O_2$, UV/$Fe^{2+}$, $Fe^{2+}$/$H_2O_2$ and UV/$Fe^{2+}$/$H_2O_2$ processes were compared in terms of percentage color and COD removal efficiency as well as electrical energy per order from the real distillery industrial effluent and the results are given in the Fig. 2. It is evident from the Fig. 2, the percentage color removal was about 12%, 22%, 18%, 67%, 50%, 58% and 96.40% and for the percentage COD removal was about 7%, 15%, 12%, 55%, 48%, 40.50%, and 83.94% by UV treatment, $H_2O_2$, $Fe^{2+}$, UV/$H_2O_2$, UV/$Fe^{2+}$, $Fe^{2+}$/$H_2O_2$ and UV/$Fe^{2+}$/$H_2O_2$ process, respectively. The results indicated that, the use of UV irradiation, $H_2O_2$ and $Fe^{2+}$ treatment alone had low color and COD removal efficiency. It is due to small amount of $^{\bullet}OH$ is formed in the presence of only UV irradiation, $H_2O_2$ and $Fe^{2+}$ [45,46]. Moderately low percentage color and COD removal efficiency was observed for UV/$H_2O_2$, UV/$Fe^{2+}$ and $Fe^{2+}$/$H_2O_2$ processes and highest percentage color and COD removal efficiency was

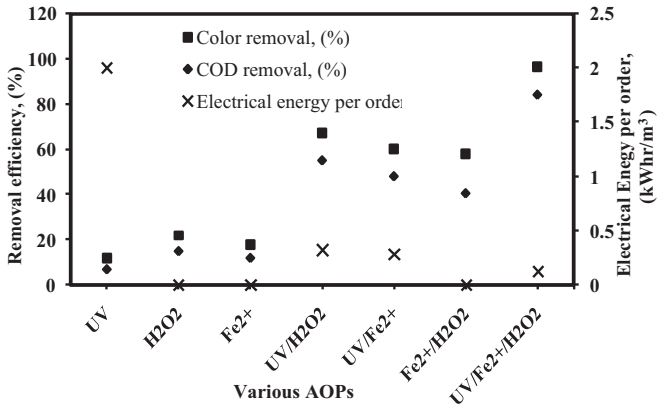


**Fig. 2.** Comparison of UV, $H_2O_2$, $Fe^{2+}$, UV/$H_2O_2$, UV/$Fe^{2+}$, $Fe^{2+}$/$H_2O_2$ and UV/$Fe^{2+}$/$H_2O_2$ process on the percentage color, COD removal and electrical energy per order (condition: $Fe^{2+}$ concentration :1.50 mM; $H_2O_2$ concentration:200 mM; effluent COD concentration:1500 mM; effluent pH: 3.2 and reaction time: 3 h).

observed by combined UV with $Fe^{2+}/H_2O_2$ process, similar observation has also been reported for the Photodegradation of Reactive Black 5, Direct Red 28 and Direct Yellowv 12 [47]. It is known that UV/$Fe^{2+}/H_2O_2$ process results in a higher hydroxyl radicals ($^{\bullet}OH$) production compared to the UV treatment, $H_2O_2$, $Fe^{2+}$, UV/$H_2O_2$, UV/$Fe^{2+}$ and $Fe^{2+}/H_2O_2$ process, thus increasing the pollutant removal efficiency in UV/$Fe^{2+}/H_2O_2$ system [48]. In UV/$Fe^{2+}/H_2O_2$ process, introduce the $Fe^{2+}$ and $H_2O_2$ into UV system led to an important increase to generate more $HO^{\bullet}$ radical in abundant quantities for an efficient pollutant removal within shorter reaction time. The reactions mechanisms involved in UV/$Fe^{2+}/H_2O_2$ process for the removal of pollutant was discussed and given bellow. The UV/$Fe^{2+}/H_2O_2$ process utilizes a combination of hydrogen peroxide ($H_2O_2$) and Ferrous ions ($Fe^{2+}$) in the presence of UV radiation. The first step of the process is the Fenton reaction [49], represented by Eq. (7).

$$Fe^{2+} + H_2O_2 \rightarrow Fe^{3+} + OH^- + {}^{\bullet}OH \quad (7)$$

In the presence of UV radiation, Ferric ions ($Fe^{3+}$) produced in thermal Fenton reaction are photocatalytically converted back to ferrous ions ($Fe^{2+}$), as shown in equation, with formation of an additional equivalent of $HO^{\bullet}$ [50].

$$Fe^{3+} + H_2O \xrightarrow{h\nu} Fe^{2+} + H^+ + HO^{\bullet} \quad (8)$$

The $HO^{\bullet}$ formed in these two reactions react with organic species (RH) present in the system, promoting their oxidation, as indicated below the equation.

$$HO^{\bullet} + RH \rightarrow H_2O + R^{\bullet} \quad (9)$$

Oscar Primo et al. observed the same trend in the comparison of photo-Fenton, Fenton-like, Fenton and UV/$H_2O_2$ process for the landfill leachate and they are report UV/$Fe^{2+}/H_2O_2$ process was to be the most efficient method [51]. It compares the electrical energy per order of different UV-based AOPs such as UV, UV/$H_2O_2$, UV/$Fe^{2+}$ and UV/$Fe^{2+}/H_2O_2$ is a measure of the electrical efficiency of AOPs system. Electrical energy per order was calculated using Eq. (4) for the removal of COD from distillery industry effluent using UV based AOPs and the results are shown in Fig. 2. According to the Fig. 2, the minimum electrical energy per order of 0.12 kW h/$m^3$ was required for the removal of 83.94% COD and 96.40% color in the UV/$Fe^{2+}/H_2O_2$ process. The UV, UV/$H_2O_2$ and UV/$Fe^{2+}$ process having higher electrical energy per order with lower removal of color and COD efficiency compared to the UV/$Fe^{2+}/H_2O_2$ process. Low electrical energy per order describes more efficient treatment methods for the removal of pollutant. So the further investigation UV/$Fe^{2+}/H_2O_2$ was studied and to obtain the UV/$Fe^{2+}/H_2O_2$ process performance by operating various parameters such as $H_2O_2$ concentration, $Fe^{2+}$ concentration, effluent COD concentration and effluent pH was studied for the removal of color and COD using response surface methodology.

### 3.2. Central Composite Design

Central Composite Design (CCD) process involves mainly four major steps: (i) Design of experiments: the determination of the independent parameters and their levels are carried out. (ii) Mathematical model developed: A mathematical model of the second order response surface with the best fittings is developed. (iii) Optimum point found: the optimal sets of experimental parameters that produce a maximum or minimum value of response are found. (iv) Response surface and contour plot: The response surface and contour plot response as a function of independent parameters and determination of optimal points are determined. In this research work, four factors and five level CCD was used to evaluate and optimize the UV/$Fe^{2+}/H_2O_2$ process variables on the responses such as percentage color and COD removal efficiency of distillery industry wastewater. The variables and levels of design model are given in Table 1. The total number of experiment with four factors was obtained as 30 run. Twenty four experiments were augmented with six replications at the design center to evaluate the pure error and were carried in randomized order as required in many design procedures. Table 2 shows number of experimental run, experimental conditions and response of percentage color and COD removal efficiency with predicted value.

#### 3.2.1. Statistical analysis and fitting of second-order polynomial equation

Experiments were performed to study the effect of $Fe^{2+}$ concentration($X_1$), $H_2O_2$ concentration($X_2$), COD concentration($X_3$) and effluent pH($X_4$) on the percentage color and COD removal efficiency using UV/$Fe^{2+}/H_2O_2$ process for the industrial effluent. The results of the percentage color ($Y_1$) and COD ($Y_2$) removal efficiency by UV/$Fe^{2+}$/H2O2 process were measured according to design matrix and measured responses are listed in Table 2. Linear, interactive, quadratic and cubic models were fitted to the experimental data to obtain the regression equations. Two different tests namely sequential model sum of squares and model summary statistics

**Table 1**
Coded and actual values of the variables of the design of experiments for the UV/$Fe^{2+}/H_2O_2$ process.

| Variable | Unit | Factors | Levels | | | | |
|---|---|---|---|---|---|---|---|
| | | | − 2 | − 1 | 0 | + 1 | + 2 |
| $Fe^{2+}$ concentration | mM | $X_1$ | 0.5 | 1 | 1.5 | 2 | 2.55 |
| $H_2O_2$ concentration | mM | $X_2$ | 50 | 100 | 150 | 200 | 250 |
| Effluent COD concentration | ppm | $X_3$ | 1000 | 2000 | 3000 | 4000 | 5000 |
| Effluent pH | – | $X_4$ | 2 | 2.5 | 3 | 3.5 | 4 |

**Table 2**
Experimental design matrix and response based on the experimental runs and predicted values on Color removal and COD removal (%) proposed by CCD design.

| Run order | $Fe^{2+}$ mM, ($X_1$) | $H_2O_2$ mM, ($X_2$) | COD ppm, ($X_3$) | Effluent pH, ($X_4$) | Color removal, (%) | | COD removal, (%) | |
|---|---|---|---|---|---|---|---|---|
| | | | | | Actual | Predicted | Actual | Predicted |
| 1 | 1.5 | 50 | 3000 | 3 | 60 | 58.39 | 44.5 | 45.25 |
| 2 | 2 | 200 | 2000 | 2.5 | 85.5 | 84.99 | 70 | 71.43 |
| 3 | 1 | 200 | 2000 | 3.5 | 85.45 | 85.21 | 70.75 | 72.12 |
| 4 | 2 | 100 | 4000 | 3.5 | 66 | 66.84 | 51 | 51.57 |
| 5 | 2 | 200 | 4000 | 3.5 | 69.5 | 68.91 | 55.25 | 56.25 |
| 6 | 1.5 | 150 | 5000 | 3 | 56.5 | 55.35 | 42 | 41.88 |
| 7 | 1.5 | 150 | 1000 | 3 | 95 | 95.13 | 83.25 | 80.92 |
| 8 | 1 | 200 | 4000 | 3.5 | 62 | 60.99 | 47.5 | 48.07 |
| 9 | 2 | 100 | 2000 | 3.5 | 84 | 83.58 | 69 | 69.25 |
| 10 | 1 | 100 | 2000 | 3.5 | 78.5 | 77.79 | 63 | 63.44 |
| 11 | 1.5 | 150 | 3000 | 3 | 83 | 83.00 | 66.5 | 66.50 |
| 12 | 1 | 100 | 2000 | 2.5 | 63.75 | 64.70 | 50 | 50.01 |
| 13 | 1.5 | 150 | 3000 | 2 | 50 | 47.93 | 34.5 | 33.73 |
| 14 | 1.5 | 150 | 3000 | 4 | 66.25 | 67.30 | 54 | 52.41 |
| 15 | 1 | 200 | 2000 | 2.5 | 75.25 | 75.08 | 62 | 62.88 |
| 16 | 1.5 | 150 | 3000 | 3 | 83 | 83.00 | 66.5 | 66.50 |
| 17 | 1 | 100 | 4000 | 2.5 | 48 | 48.46 | 34.5 | 34.08 |
| 18 | 2.5 | 150 | 3000 | 3 | 90.5 | 89.43 | 75 | 72.92 |
| 19 | 1.5 | 150 | 3000 | 3 | 83 | 83.00 | 66.5 | 66.50 |
| 20 | 1.5 | 150 | 3000 | 3 | 83 | 83.00 | 66.5 | 66.50 |
| 21 | 1 | 200 | 4000 | 2.5 | 51.25 | 52.04 | 40.75 | 41.51 |
| 22 | 1.5 | 150 | 3000 | 3 | 83 | 83.00 | 66.5 | 66.50 |
| 23 | 0.5 | 150 | 3000 | 3 | 73 | 73.05 | 58 | 57.63 |
| 24 | 1 | 100 | 4000 | 3.5 | 59.5 | 60.37 | 45.25 | 44.83 |
| 25 | 2 | 100 | 4000 | 2.5 | 57 | 57.60 | 42.5 | 42.14 |
| 26 | 2 | 200 | 4000 | 2.5 | 61.25 | 62.63 | 50 | 51.00 |
| 27 | 1.5 | 250 | 3000 | 3 | 70.25 | 70.84 | 66 | 62.79 |
| 28 | 2 | 100 | 2000 | 2.5 | 71.5 | 73.17 | 56.25 | 57.13 |
| 29 | 2 | 200 | 2000 | 3.5 | 92.25 | 92.45 | 77.5 | 79.36 |
| 30 | 1.5 | 150 | 3000 | 3 | 83 | 83.00 | 66.5 | 66.50 |

were employed to decide about the adequacy of various models to represent percentage color and COD removal efficiency by UV/$Fe^{2+}$/$H_2O_2$ process. Results of these tests are given in Tables 3 and 4, for percentage color and COD removal efficiency, respectively. It can be seen from the Tables 3 and 4, the cubic model was found to be aliased. For quadratic and linear models, *p* value was lower than 0.02, and both of these model could be used for further study as per sequential model sum of squares test. As per model summary statistics results is given in Tables 3 and 4, the quadratic model was found to have maximum "*Adjusted* $R^2$" and "*Predicted* $R^2$" values excluding cubic model which was aliased (Tables 3 and 4). Therefore, quadratic model was chosen for further analysis.

**Table 3**
Sequential model sum of squares and model summary statistics for % color removal.

**Sequential model sum of squares**

| Source | Sum of squares | df | Mean square | F Value | p-value Prob > F | |
|---|---|---|---|---|---|---|
| Mean vs Total | 1.570E + 005 | 1 | 1.570E + 005 | | | |
| Linear vs Mean | 3571.80 | 4 | 892.95 | 13.85 | < 0.0001 | |
| 2FI vs Linear | 66.04 | 6 | 11.01 | 0.14 | 0.9899 | |
| Quadratic vs 2FI | 1523.80 | 4 | 380.95 | 265.89 | < 0.0001 | Suggested |
| Cubic vs Quadratic | 18.25 | 8 | 2.28 | 4.93 | 0.0247 | Aliased |
| Residual | 3.24 | 7 | 0.46 | | | |
| Total | 1.622E + 005 | 30 | 5405.85 | | | |

**Model summary statistics**

| Source | Std. Dev. | R-Squared | Adjusted R-Squared | Predicted R-Squared | Press | |
|---|---|---|---|---|---|---|
| Linear | 8.03 | 0.6891 | 0.6394 | 0.5790 | 2182.01 | |
| 2FI | 9.02 | 0.7019 | 0.5449 | 0.4869 | 2659.62 | |
| Quadratic | 1.20 | 0.9959 | 0.9920 | 0.9761 | 123.79 | Suggested |
| Cubic | 0.68 | 0.9994 | 0.9974 | 0.9099 | 466.83 | Aliased |

**Table 4**
Sequential model sum of squares and model summary statistics for % COD removal.

| **Sequential model sum of squares** | | | | | | |
|---|---|---|---|---|---|---|
| **Source** | **Sum of squares** | **df** | **Mean square** | **F value** | **p-value Prob > F** | |
| Mean vs Total | 1.011E + 005 | 1 | 1.011E + 005 | | | |
| Linear vs Mean | 3622.02 | 4 | 905.50 | 18.81 | < 0.0001 | |
| 2FI vs Linear | 58.99 | 6 | 9.83 | 0.16 | 0.9836 | |
| Quadratic vs 2FI | 1107.65 | 4 | 276.91 | 112.55 | < 0.0001 | Suggested |
| Cubic vs Quadratic | 18.67 | 8 | 2.33 | 0.90 | 0.5643 | Aliased |
| Residual | 18.24 | 7 | 2.61 | | | |
| Total | 1.059E+005 | 30 | 3531.00 | | | |
| **Model summary statistics** | | | | | | |
| **Source** | **Std. Dev.** | **R-Squared** | **Adjusted R-Squared** | **Predicted R-Squared** | **PRESS** | |
| Linear | 6.94 | 0.7506 | 0.7107 | 0.6540 | 1669.77 | |
| 2FI | 7.76 | 0.7628 | 0.6380 | 0.5696 | 2076.96 | |
| Quadratic | 1.57 | 0.9924 | 0.9852 | 0.9559 | 212.58 | Suggested |
| Cubic | 1.61 | 0.9962 | 0.9843 | 0.4558 | 2625.94 | Aliased |

### *3.2.2. Evaluation of experimental results with design of experiments*

A four factor and five levels CCD was applied to optimize the mutual effects of four independent variables such as $Fe^{2+}$ concentration($X_1$), $H_2O_2$ concentration ($X_2$), effluent COD concentration($X_3$) and effluent pH($X_4$) on the percentage color and COD removal efficiency. The design of experiment and the results of the RSM tests are listed in the Table 2. According to the results of RSM, a second order polynomial regression equation for describing the percentage color ($Y_1$) and COD ($Y_2$) removal efficiency can be expresses as follows.

$$\textit{Color}\ \text{removal},\ (\%)Y_1 = 83 + 40.10X_1 + 30.11X_2 - -90.95X_3 + 40.84X_4 + 00.36X_1X_2 + 00.17X_1X_3 - 00.67X_1X_4 - 10.70X_2X_3 - 00.74X_2X_4 - 00.29X_3X_4 - 00.44X_1^2 - 40.60X_2^2 - 10.94X_3^2 - 60.35X_4^2 \quad (10)$$

$$\textit{COD}\ \text{removal},\ (\%)\ Y_2 = 660.50 + 30.82X_1 + 40.39X_2 - 90.77X_3 + 40.67X_4 + 00.36X_1X_2 + 00.23X_1X_3 - 00.33X_1X_4 - 10.36X_2X_3 - 10.05X_2X_4 - 00.67X_3X_4 - 00.31X_1^2 - 30.12X_2^2 - 10.28X_3^2 - 50.86X_4^2 \quad (11)$$

**Table 5**
ANOVA of the second-order polynomial equation for % color removal.

| **ANOVA for response surface quadratic model** | | | | | | |
|---|---|---|---|---|---|---|
| **Source** | **Sum of squares** | **df** | **Mean square** | **F value** | **p-value Prob > F** | |
| Model | 5161.63 | 14 | 368.69 | 257.34 | < 0.0001 | Highly significant |
| $X_1$-$Fe^{2+}$ concentration | 402.62 | 1 | 402.62 | 281.02 | < 0.0001 | Highly significant |
| $X_2$-$H_2O_2$ concentration | 232.50 | 1 | 232.50 | 162.28 | < 0.0001 | Highly significant |
| $X_3$-COD concentration | 2374.07 | 1 | 2374.07 | 1657.05 | < 0.0001 | Highly significant |
| $X_4$-effleunt pH | 562.60 | 1 | 562.60 | 392.68 | < 0.0001 | Highly significant |
| $X_1X_2$ | 2.10 | 1 | 2.10 | 1.47 | 0.2445 | |
| $X_1X_3$ | 0.46 | 1 | 0.46 | 0.32 | 0.5811 | |
| $X_1X_4$ | 7.16 | 1 | 7.16 | 4.99 | 0.0411 | significant |
| $X_2X_3$ | 46.24 | 1 | 46.24 | 32.27 | < 0.0001 | Highly significant |
| $X_2X_4$ | 8.70 | 1 | 8.70 | 6.07 | 0.0263 | significant |
| $X_3X_4$ | 1.38 | 1 | 1.38 | 0.96 | 0.3418 | |
| $X_1^2$ | 5.33 | 1 | 5.33 | 3.72 | 0.0730 | |
| $X_2^2$ | 579.60 | 1 | 579.60 | 404.55 | < 0.0001 | Highly significant |
| $X_3^2$ | 103.30 | 1 | 103.30 | 72.10 | < 0.0001 | Highly significant |
| $X_4^2$ | 1104.90 | 1 | 1104.90 | 771.20 | < 0.0001 | Highly significant |
| Residual | 21.49 | 15 | 1.43 | | | |
| Lack of Fit | 21.49 | 10 | 2.15 | | | |
| Pure Error | 0.000 | 5 | 0.000 | | | |
| Cor Total | 5183.12 | 29 | | | | |

Coefficient of Variance = 1.65; adequate precision = 55.767.

**Table 6**
ANOVA of the second-order polynomial equation for % COD removal.

| ANOVA for response surface quadratic model | | | | | | |
|---|---|---|---|---|---|---|
| **Source** | **Sum of squares** | **df** | **Mean square** | **F Value** | **p-value Prob > F** | |
| Model | 4788.66 | 14 | 342.05 | 139.02 | < 0.0001 | Highly significant |
| $X_1$-$Fe^{2+}$ Concentration | 350.75 | 1 | 350.75 | 142.56 | < 0.0001 | Highly significant |
| $X_2$-$H_2O_2$ Concentration | 461.57 | 1 | 461.57 | 187.59 | < 0.0001 | Highly significant |
| $X_3$-COD concentration | 2286.38 | 1 | 2286.38 | 929.25 | < 0.0001 | Highly significant |
| $X_4$-effluent pH | 523.32 | 1 | 523.32 | 212.69 | < 0.0001 | Highly significant |
| $X_1X_2$ | 2.07 | 1 | 2.07 | 0.84 | 0.3739 | |
| $X_1X_3$ | 0.88 | 1 | 0.88 | 0.36 | 0.5590 | |
| $X_1X_4$ | 1.72 | 1 | 1.72 | 0.70 | 0.4159 | |
| $X_2X_3$ | 29.57 | 1 | 29.57 | 12.02 | 0.0035 | Significant |
| $X_2X_4$ | 17.54 | 1 | 17.54 | 7.13 | 0.0175 | Significant |
| $X_3X_4$ | 7.22 | 1 | 7.22 | 2.94 | 0.1072 | |
| $X_1^2$ | 2.58 | 1 | 2.58 | 1.05 | 0.3223 | |
| $X_2^2$ | 266.84 | 1 | 266.84 | 108.45 | < 0.0001 | Highly significant |
| $X_3^2$ | 44.61 | 1 | 44.61 | 18.13 | 0.0007 | Highly significant |
| $X_4^2$ | 941.18 | 1 | 941.18 | 382.53 | < 0.0001 | Highly significant |
| Residual | 36.91 | 15 | 2.46 | | | |
| Lack of Fit | 36.91 | 10 | 3.69 | | | |
| Pure Error | 0.000 | 5 | 0.000 | | | |
| Cor Total | 4825.57 | 29 | | | | |

Coefficient of Variance = 2.70; adequate precision = 42.546.

### 3.2.3. Adequacy of the model tested for percentage color and COD removal

Analysis of variance was carried out to justify the significance and adequacy of the regression model and the results are summarized in Tables 5 and 6. The model *F*-value for percentage color and COD removal were about 257.34 and 139.02, respectively, the value indicating that the models were highly adequate and significant. Furthermore, the determination coefficients ($R^2$) of the models were 0.9959 and 0.9924 for color and COD removal, respectively, which indicated that prediction of color and COD removal efficiency by the polynomial model was excellent. Moreover, the F-values for lack of fit of 21.49 for color removal and 36.91 for COD removal implied that the lack of fit was significant. There is only a 0.01% for color removal and 0.01% for COD removal chance that a lack of fit *F*-value this large could occur due to noise. Furthermore, a relatively low value of the coefficient of variation (CV, %) in Tables 5 and 6 apparently showed that variation was acceptable and satisfactory. In addition, adequate precision can be used to measure the signal to noise ratio. Desirable ratios of 55.76 for color removal and 42.54 for COD removal implied an adequate signal. Therefore, the models could be applied to navigate the design space. The values of all regression coefficients with the significance levels were given in Tables 5 and 6. It could be seen from the Table 5 for the percentage color removal efficiency, the linear coefficients of $Fe^{2+}$ concentration($X_1$), $H_2O_2$ concentration($X_2$), COD concentration($X_3$) and effluent pH($X_4$) and the interaction effect of $Fe^{2+}$ concentration($X_1$)xeffluent pH($X_4$), $H_2O_2$ concentration($X_2$)xCOD concentration($X_3$), $H_2O_2$ concentration($X_2$)xeffluent pH ($X_4$) as well as the quadratic coefficient of $H_2O_2$ concentration($X_2^2$), COD concentration($X_3^2$) and effluent pH ($X_4^2$) are significant factors and for the percentage COD removal efficiency (Table 6), the linear coefficients of $Fe^{2+}$ concentration ($X_1$), $H_2O_2$ concentration($X_2$), COD concentration($X_3$) and effluent pH($X_4$) and the interaction effect of $H_2O_2$ concentration($X_2$)xCOD concentration ($X_3$), $H_2O_2$ concentration($X_2$)xeffluent pH ($X_4$) as well as the quadratic coefficient of $H_2O_2$ concentration($X_2^2$), COD concentration ($X_3^2$) and effluent pH($X_4^2$) are significant factors at a level less than 5%. The ANOVA analysis shows that the form of the model chosen to explain the relationship between the factors and the response is correct [32]. Accuracy of the data could be examined by constructing a normal probability plot of the residuals. Normally, the residuals distributed points in the plot should follow a straight line. Fig. 3(a) and (b) illustrates the normal probability plot of residual values for the percentage color and COD removal efficiency, respectively. There was no apparent problem with normality and no requirement for response transformation. The studentized residual versus predicted values are shown in Fig. 4(a) and (b) for the percentage color and COD removal efficiency; the random scatter of the residuals (above and below the centerline) indicated that the model for color and COD removal was significant. Furthermore, the Fig. 5(a) and (b) showed that the actual versus predicted values of color and COD removal efficiency approximately fit the 45° line, demonstrates that the quadratic model was appropriate in fitting the color and COD removal efficiency for the experimental data. The above results illustrated the accuracy and applicability of the central composite design model for color and COD removal process optimization.

### 3.3. Combined effect of operating parameters for percentage color and COD removal efficiency

Three dimensional response surface plots are plotted using developed mathematical models in order to study the individual and interactive effect among the process variables on the responses and also used to determine the optimal condition of each factor for maximum removal efficiency of color and COD.

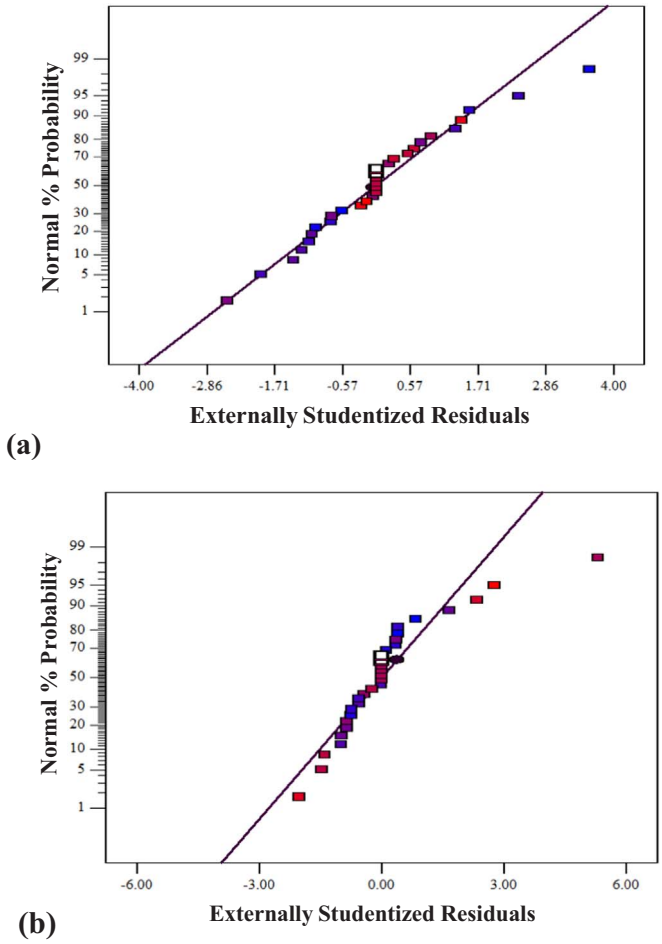


**Fig. 3.** Plot for relationship between normal % probability and external studentized residuals for (a) % color removal and (b) % COD removal.

### *3.3.1. Effect of $H_2O_2$ and $Fe^{2+}$ concentration*

In the photo - Fenton processes, concentration of $H_2O_2$ and $Fe^{2+}$ play very important parameters in terms of overall cost process removal efficiency and largely responsible for generation of hydroxyl radicals [25,31]. The important parameters such as effect dosage of $H_2O_2$ and $Fe^{2+}$ concentration on color and COD removal efficiency was investigated by UV/$Fe^{2+}$/$H_2O_2$ process for the distillery industrial wastewater and the results are given in Table 2 and shown in Fig. 6(a) and (b). Fig. 6(a) and (b) shows that the combined effects of $H_2O_2(X_2)$ and $Fe^{2+}(X_1)$ concentration on the percentage color and COD removal efficiency at a constant amount of effluent COD concentration of 3000 ppm, effluent pH of 3 and reaction time of 3 h. The both % color and COD removal efficiency was increased with increasing of $H_2O_2(X_2)$ concentration ranging from 50 to 200 mM and then slightly decreased, when further increasing $H_2O_2(X_2)$ concentration from 200 to 250 mM, at any value of $Fe^{2+}$ concentration($X_1$). The increasing trend in the color and COD removal efficiency is due to the increase in hydroxyl radical ($^{\bullet}OH$) concentration by addition of $H_2O_2$ concentration. The slightly decreases is due to that the fact that at a higher $H_2O_2$ concentration scavenging of hydroxyl radicals ($^{\bullet}OH$) will occur, which can be expressed by the following equations [25].

$$HO^{\bullet} + H_2O_2 \rightarrow H_2O + HO_2^{\bullet} \quad (12)$$

$$HO_2^{\bullet} + HO^{\bullet} \rightarrow H_2O + O_2 \quad (13)$$

$$HO^{\bullet} + HO^{\bullet} \rightarrow H_2O_2 \quad (14)$$

The reduction potential of $HO_2^{\bullet}$ is much lower (1.0 V) than that of $HO^{\bullet}$ (2.8 V) and this is most probably the reason for decrease in color and COD removal efficiency [52]. Similar observation has also been observed [25].

The effect of $H_2O_2$ concentration on electrical energy per order has been studied and the results are shown in Fig. 7. As it can be seen from the Fig. 7, when $H_2O_2$ concentration was increased from 50 to 200 mM, the electrical energy per order was decreased from 0.37 to 0.13 kW h/$m^3$, it is due to the generation of more hydroxyl radicals with increasing $H_2O_2$ concentration; however when the $H_2O_2$ concentration increasing from 200 to 250 mM, the electrical energy per order was increased from 0.13 to 0.21 kW h/$m^3$. This is may be due to fact that the coincident hydroxyl radicals at higher concentration of $H_2O_2$ [29].

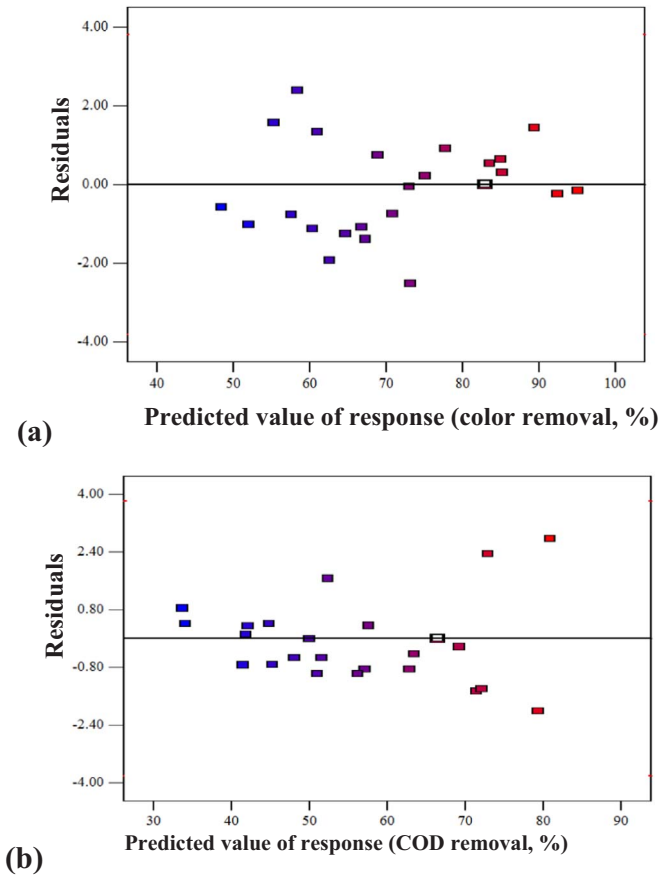


**Fig. 4.** Plot for relationship between residuals and predicted values response for (a) % color removal and (b) % COD removal.

Effect of $Fe^{2+}$($X_1$) concentration on the removal color and COD removal efficiency was investigated using the photo-Fenton process in the range of from 0.5 to 2.5 mM and the results are shown in Fig. 6(a) and (b). It was found that from Fig. 6(a) and (b), color and COD removal efficiency was increased with increasing the initial $Fe^{2+}$ concentration at any value of $H_2O_2$ concentration ($X_2$) and the higher color and COD was obtained with 2 mM. However, further increases in $Fe^{2+}$ initial concentration showed no further color and COD removal due to the fact that $HO^{\bullet}$ – scavenging reactions became more and more dominant at excessive $Fe^{2+}$concentrations [53] according to reaction (15) and (16) [25].

$$H_2O_2 + HO^{\bullet} \rightarrow H_2O^{-} + HO_2^{\bullet} \quad (15)$$

$$Fe^{2+} + HO^{\bullet} \rightarrow OH^{-} + Fe^{3+} \quad (16)$$

The effect of $Fe^{2+}$ concentration on electrical energy per order was also calculated for removal of color and COD from distillery industry wastewater using the UV/$Fe^{2+}$/$H_2O_2$ process and the results are shown in the Fig. 8. From the Fig. 8, the electrical energy per order decreased from 0.25 to 0.14 kW h/$m^3$, when the increasing $Fe^{2+}$ concentration from 0 to 2.0 mM, further increasing $Fe^{2+}$ concentration from 2.0 to 2.5 mM, the electrical energy per order was increased from 0.14 to 0.16 kW h/$m^3$. According to our results indicate that optimum level of $Fe^{2+}$ and $H_2O_2$ concentration in UV/$Fe^{2+}$/$H_2O_2$ process produce more hydroxyl radicals comparing with other experimental conditions [29].

### *3.3.2. COD concentration and effluent pH*

The initial COD concentration of effluent and initial effluent pH in a given UV/$Fe^{2+}$/$H_2O_2$ process is important factor which is needs to be taken into account [54]. The combined effect of effluent COD concentration($X_3$) and effluent pH($X_4$) with constant amount of $H_2O_2$ of 150 mM, and $Fe^{2+}$ concentration of 1.5 mM with reaction time of 3 h on the percentage color and COD removal was studied using the UV/$Fe^{2+}$/$H_2O_2$ process for the distillery industrial effluent and the results are given in the Table 2 and shown in Fig. 9(a) and (b). The influence of COD concentration on removal of percentage color and COD efficiency is shown in Fig. 9(a) and (b). From the Fig. 9(a) and (b) it is possible to see that the extent of color and COD removal decreases with the increasing effluent COD concentration from 1000 to 5000 ppm. The increase in effluent COD concentration, which means that increases number of organic molecules and not the $HO^{\bullet}$ radical concentration, so percentage color and COD removal efficiency was decreased. In any photochemical process at high effluent concentration, the penetration of photons entering into solution decreases thereby was

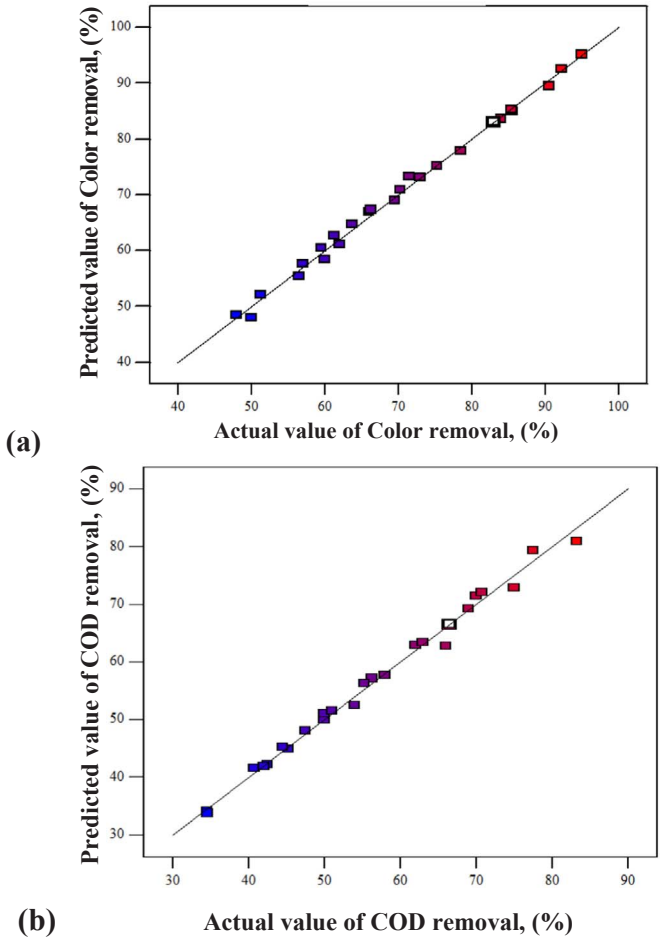


**Fig. 5.** Plot for relationship between actual and predicted value for (a) % color removal and (b) % COD removal.

lowering the •OH concentration. Consequently, the removal of pollutant was decreased with increasing effluent COD concentration [55,56]. Effect of COD concentration on electrical energy per order was also investigated and the results are shown in the Fig. 10. It is evident from the Fig. 10 the electrical energy per order was increased from 0.12 to 0.40 kW h/$m^3$ with increasing effluent COD concentration from 1000 to 5000 ppm. This is may be due to that the less production of •OH with increasing effluent COD concentration.

Reaction pH is one of the most important process parameters in the Fenton and photo-Fenton processes, since iron speciation which in turn determines the UV absorption, complexation, and dissolution properties of the catalyst, is strongly affected by solution pH [57]. The most suitable pH range for the removal of organic pollutants with the Fenton and photo-Fenton processes has already been established as 2–5 [25,58,59]. The effect of initial effluent pH on the percentage color and COD removal efficiency was studied and the results are shown in the Fig. 9(a) and (b). It can be ascertained from the Fig. 9(a) and (b) the efficiency color and COD removal was increased with increasing effluent pH from 2 to 3. However, the effluent pH changing from 3 to 4, the percentage color and COD removal was decreased, these results are in agreement with those reported in previous studies [25]. The major reactions of the formation of HO• in the photo-Fenton process include Fenton reaction, photolysis of hydrogen peroxide and photo reduction of ferric ion, as shown in Eqs. (7), (8) and (17), respectively.

$$H_2O_2 + UV \rightarrow 2HO^{\bullet} \tag{17}$$

As indicated in Eq. (7), the amount of HO• formed through Fenton process is affected by pH. The HO• can be efficiently formed especially under acidic condition. The optimal pH of Fenton and photo-Fenton process was around 3 [60] because the main species at pH 2–3, $Fe(OH)_2{}^+(H_2O)^5$, is the one with the largest light absorption coefficient and quantum yield for •OH radical production.

Effect of effluent pH on electrical energy per was investigated and the results are shown in Fig. 11. It is evident from the Fig. 11, the electrical energy per order was decreased from 0.53 to 0.20 kW h/$m^3$ with increasing effluent pH from 2 to 3, however, further increasing effluent pH from 3 to 4, the electrical energy per order increased from 0.20 to 0.28 kW h/$m^3$. The above results indicating that at effluent pH 3, in this condition produce more hydroxyl radicals. Consequently, the effluent pH 3 gives low electrical energy per order and also gives higher removal of color and COD with other condition.

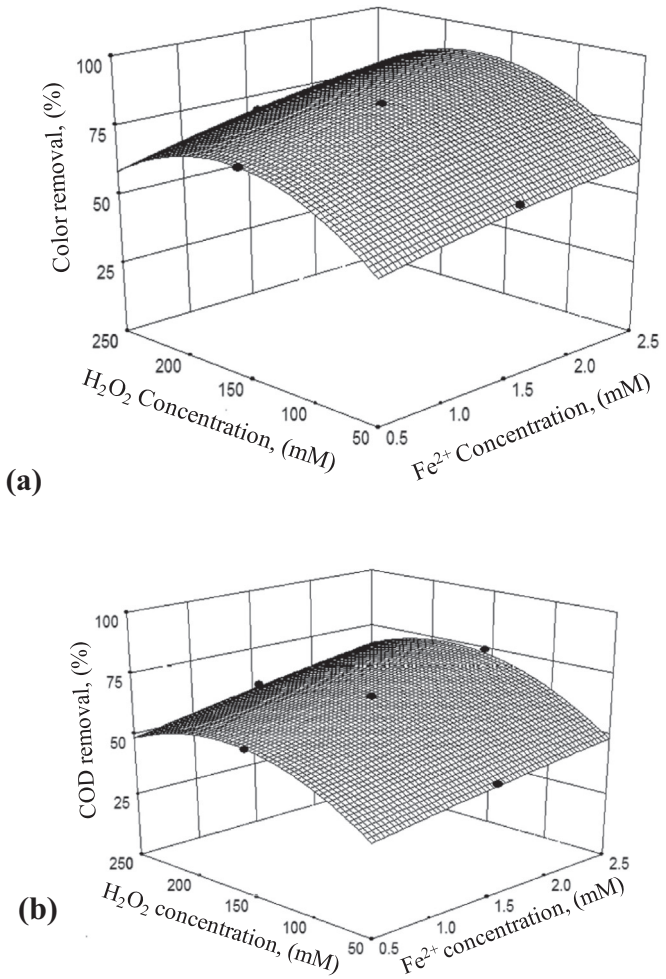


**Fig. 6.** Response surface plots for the effects of $Fe^{2+}$ concentration ($X_1$) and $H_2O_2$ concentration ($X_2$) on the (a) % color removal and (b) % COD removal (condition: COD concentration:3000 ppm; effluent pH:3; reaction time: 3 h).

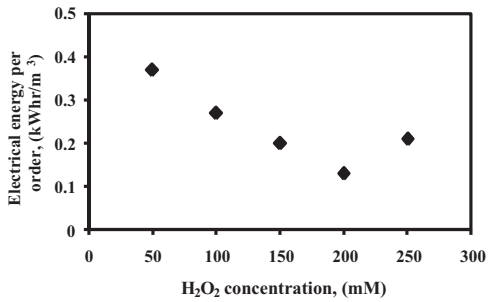


**Fig. 7.** Effect of $H_2O_2$ concentration on electrical energy per order by UV/$Fe^{2+}$/$H_2O_2$ process (condition: $Fe^{2+}$ concentration: 2 mM; COD concentration: 3000 ppm; effluent pH: 3; reaction time: 3 h).

### *3.4. Optimization*

One of the main purposes of this investigation is to obtain the optimal conditions for the percentage color and COD removal efficiency from industrial wastewater using UV/$Fe^{2+}$/$H_2O_2$ process. The results were optimized using the regression equation of RSM. In the optimization of $Fe^{2+}$ concentration($X_1$), $H_2O_2$ concentration($X_2$), effluent COD concentration($X_3$) and effluent pH($X_4$) were selected as within range and the responses such as color ($Y_1$) and COD ($Y_2$) removal efficiency was maximized. Under these optimum conditions such as $Fe^{2+}$ concentration($X_1$) -1.50 mM, $H_2O_2$ concentration($X_2$)-200 mM, effluent COD concentration($X_3$)-1500 mM and effluent pH($X_4$)-3.2, the percentage removal of color and COD was found to be 96.5% and 84%, respectively which are validated by conducting additional experiments under the above optimal conditions. A mean value of 96.40% for color removal and 83.94% for COD removal are obtained

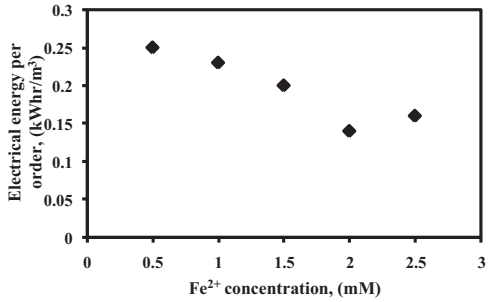


**Fig. 8.** Effect of $Fe^{2+}$ concentration on electrical energy per order by UV/$Fe^{2+}$/$H_2O_2$ process (condition: $H_2O_2$ concentration: 200 mM; COD concentration: 3000 ppm; effluent pH:3; reaction time: 3 h).

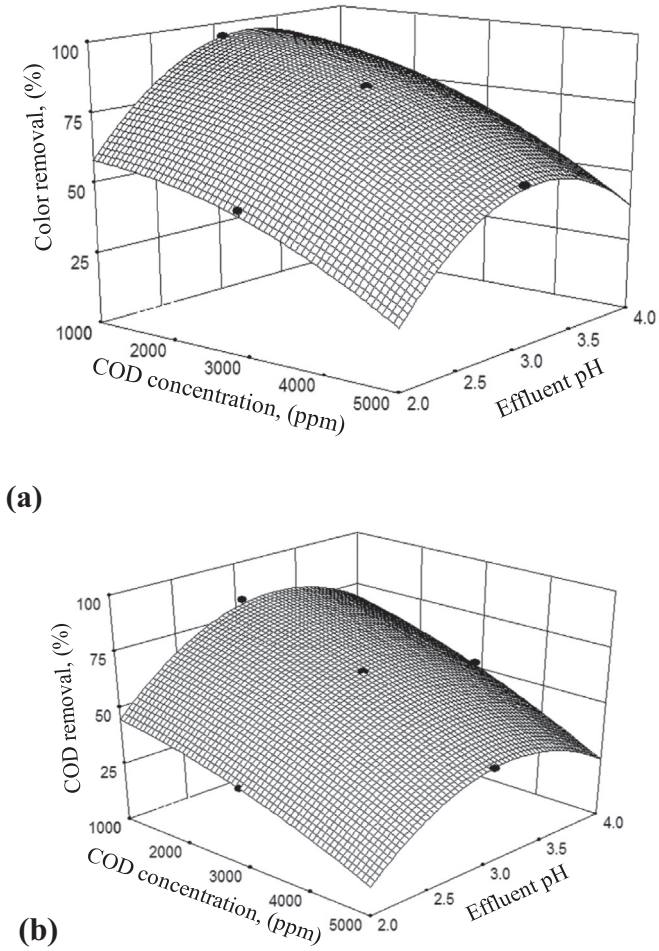


**Fig. 9.** Response surface plots for the effects of effluent COD concentration ($X_3$) and effluent initial pH ($X_4$) on the (a) % color removal and (b) % COD removal (condition: $Fe^{2+}$ concentration: 1.5 mM; $H_2O_2$ concentration: 150 mM; reaction time: 3 h).

from the experimental, which is in close agreement with the predicted values obtained. The good correlation between these actual results and predicted results indicate that the reliability of CCD incorporate desirability function method and it could be effectively used to optimize the UV/$Fe^{2+}$/$H_2O_2$ process parameters for any types of industrial effluent [61].

## 4. Instrumental analysis

Fig. 12. shows that the UV/Vis spectra (Spectroquant Pharo® 300) of distillery industry wastewater at different photochemical reaction time intervals. The absorption peak decreased with increasing photochemical reaction time. The position of the absorbance peak also changes from 302 nm to 262 nm which is indicating that, the new byproducts are formed and also the decolorization and degradation was occurred.

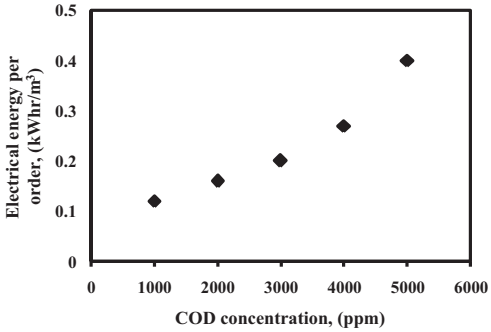


**Fig. 10.** Effect of COD concentration on electrical energy per order by UV/$Fe^{2+}$/$H_2O_2$ process (condition: $Fe^{2+}$ concentration: 2 mM; $H_2O_2$ concentration: 200 mM; effluent pH: 3; reaction time: 3 h).

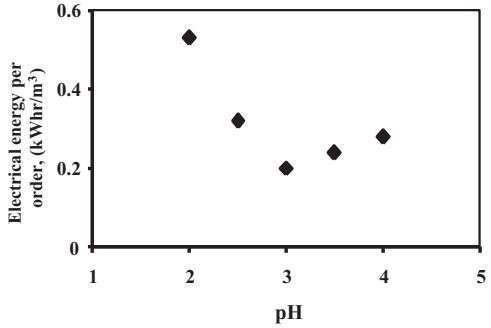


**Fig. 11.** Effect of effluent pH on electrical energy per order by UV/$Fe^{2+}$/$H_2O_2$ process (condition: $Fe^{2+}$ concentration: 2 mM; $H_2O_2$ concentration: 200 mM; COD concentration: 3000 ppm; reaction time: 3 h).

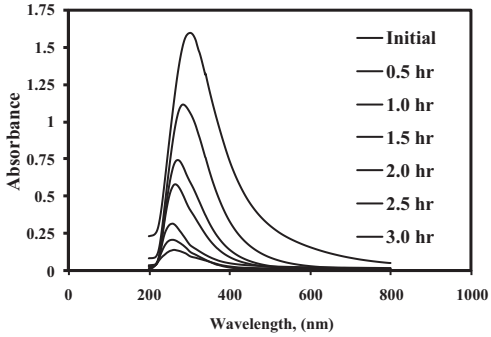


**Fig. 12.** UV/Vis spectra of distillery industrial effluent, using UV/$Fe^{2+}$/$H_2O_2$ process at different reaction time.

## 5. Conclusion

In the present experimental work, treatment of distillery industry wastewaters by different AOPs such as UV, $H_2O_2$, $Fe^{2+}$, UV/$H_2O_2$, UV/$Fe^{2+}$, $Fe^{2+}$/$H_2O_2$ and UV/$Fe^{2+}$/$H_2O_2$ process has been studied. According to our results of the present studies showed that UV/$Fe^{2+}$/$H_2O_2$ process was an efficient method for the removal color and COD with lower electrical energy per order from distillery industry wastewater. The use of response surface methodology involving central composite design for optimization of process parameters was studied. Experiments were performed as a function of $Fe^{2+}$ concentration($X_1$), $H_2O_2$ concentration($X_2$), effluent COD concentration($X_3$) and effluent pH($X_4$), these factors are well studied and optimized. The second-order polynomial regression model with high determination coefficients suggested a good fit of the model to the experimental data. The optimized values, at which the highest percentage color (96.50%) and COD (84.40%) removal was attained with low electrical energy per order of 0.12 kWhr/$m^3$, are achieved: $Fe^{2+}$ concentration − 1.50 mM, $H_2O_2$ concentration – 200 mM, effluent COD concentration – 1500 ppm and effluent pH-3.2. The experimental results demonstrated that RSM was suitable for optimizing the operation parameters for color and COD removal by UV/$Fe^{2+}$/$H_2O_2$ from industrial effluent. The coupled UV/$Fe^{2+}$/H2O2 system appears as a promising process for the removal of pollutant from any industrial effluent.

## Acknowledgements

The authors are grateful to the University of Malaya High Impact Research Grant (HIR-MOHE-D000037-16001) from the Ministry of Higher Education Malaysia which financially supported this work.

## References

[1] K. Balapure, K. Jain, N. Bhatt, D. Madamwar, Exploring bioremediation strategies to enhance the mineralization of textile industrial wastewater through sequential anaerobic-microaerophilic process, Int. Biodeterior. Biodegrad. 106 (2016) 97–105.
[2] M. Diao, N. Ouédraogo, L. Baba-Moussa, P.W. Savadogo, A.G.N. Guessan, I.H.N. Bassolé, M.H. Dicko, Biodepollution of wastewater containing phenolic compounds from leather industry by plant peroxidases, Biodegradation 22 (2) (2011) 389–396.
[3] L. Tahrani, L. Soufi, I. Mehri, A. Najjari, A. Hassan, J. Van Loco, T. Reyns, A. Cherif, H. Ben Mansour, Isolation and characterization of antibiotic-resistant bacteria from pharmaceutical industrial wastewaters, Microb. Pathog. 89 (2015) 54–61.
[4] R. Shankar, L. Singh, P. Mondal, S. Chand, Removal of COD, TOC, and color from pulp and paper industry wastewater through electrocoagulation, Desalin. Water Treat. 52 (40–42) (2014) 7711–7722.
[5] S. Basu, S. Mukherjee, A. Kaushik, V.S. Batra, M. Balakrishnan, Integrated treatment of molasses distillery wastewater using microfiltration (MF), J. Environ. Manag. 158 (2015) 55–60.
[6] C. David, M. Arivazhagan, F. Tuvakara, ecolorization of distillery spent wash effluent by electro oxidation (EC and EF) and Fenton processes: a comparative study, Ecotoxicol. Environ. Saf. 121 (2015) 142–148.
[7] S.M. Reza Razavi, T. Miri, A real petroleum refinery wastewater treatment using hollow fiber membrane bioreactor (HF-MBR), J. Water Process Eng. 8 (2015) 136–141.
[8] K.P. Yee Shak, T.Y. Wu, Coagulation–flocculation treatment of high-strength agro-industrial wastewater using natural Cassia obtusifolia seed gum: treatment efficiencies and flocs, Chem. Eng. J. 256 (2014) 293–305.
[9] I. Petrinic, J. Korenak, D. Povodnik, C. Hélix-Nielsen, A feasibility study of ultrafiltration/reverse osmosis (UF/RO)-based wastewater treatment and reuse in the metal finishing, J. Clean. Prod. 01 (2015) 292–300.
[10] J.M. Monteagudo, A. Durán, I. San Martín, S. García, Ultrasound-assisted homogeneous photocatalytic degradationof Reactive Blue 4 in aqueous solution, Appl. Catal. B 152–153 (2014) 59–67.
[11] M. Kheir-eddine Bouchareb, M. Bouhelassa, M. Berkani, Optimization of photocatalytic decolorization of C.I. Basic Blue 41 in semi-pilot scale prototype solar photoreactor, J. Chem. Technol. Biotechnol. 89 (2014) 1211–1218.
[12] I.K. Konstantinou, T.A. Albanis, Photocatalytic transformation of pesticides in aqueous titanium dioxide suspensions using artificial and solar light: intermediates and degradation pathways, Appl. Catal. B: Environ. 42 (2003) 319–335.
[13] I.K. Konstantinou, T.A. Albanis, $TiO_2$-assisted photocatalytic degradation of azo dyes in aqueous solutions: kinetic and mechanistic investigations, A review, Appl. Catal. B: Environ. 49 (2004) 1–14.
[14] I.K. Konstantinou, V.A. Sakkas, T.A. Albanis, Photocatalyticdegradation of the herbicides propanil and molinate over aqueous $TiO_2$ suspensions. Identification of intermediates and the reaction pathway, Appl. Catal. B: Environ. 34 (2001) 227–239.
[15] A. Xu, M. Yang, H. Yao, H. Du, C. Sun, Rectorite as catalyst for wet air oxidation of phenol, Appl. Clay Sci. 43 (2009) 435–438.
[16] C. Kalyanaraman, B. Kameswari, J. Raghava Rao, Studies on enhancing the biodegradation of tannins by ozonation and Fenton's oxidation process, J. Ind. Eng. Chem. 25 (2015) 329–337.
[17] R.F.F. Pontes, J.E.F. Moraes, A. Machulek, J.M. Pinto, A mechanistic kinetic model for phenol degradation by the Fenton process, J. Hazard. Mater. 176 (2010) 402–413.
[18] M. Hongzhu, X. Zhang, M. Qingliang, B. Wang, Electro chemical catalytic treatment of phenol wastewater, J. Hazard. Mater. 165 (2009) 475–481.
[19] H. Feng, L. Le-cheng, Degradation kinetics and mechanisms of phenol in photo-Fenton process, J. Zhejiang Univ. Sci. 5 (2004) 198–205.
[20] B.H. Diya'uddeen, A.R. Abdul Aziz, W.M. Ashri Wan Daud, Oxidative mineralisation of petroleum refinery effluent using Fenton-like process, Chem. Eng. Res. Des. 90 (2012) 298–307.
[21] A. Babuponnusami, K. Muthukumar, Degradation of phenol in aqueous solution by Fenton, sono-Fenton and sono–photo-Fenton methods, J. Clean. Soil Air Water 39 (2011) 142–147.
[22] M. Neamtu, A. Yediler, I. Siminiceanu, A. Kettrup, Oxidation of commercial reactive azo dye aqueous solutions by the photo-Fenton and Fenton-like processes, J. Photochem. Photobiol. A. 161 (2003) 87–93.
[23] H. Katsumata, S. Kawabe, S. Kaneco, T. Suzuki, K. Ohta, Degradation of bisphenol A in water by the photo-Fenton reaction, J. Photochem. Photobiol. A. 162 (2004) 297–305.
[24] H. Katsumata, S. Kaneco, T. Suzuki, K. Ohta, Y. Yobiko, Photo-Fenton degradation of alachlor in the presence of citrate solution, J. Photochem. Photobiol. A 180 (2006) 38–45.
[25] M.S. Lucas, J.A. Peres, Decolorization of the azo dye Reactive Black 5 by Fenton and photo-Fenton oxidation, Dyes Pigm. 71 (2006) 236–244.
[26] T.M. Elmorsi, Y.M. Riyad, Z.H. Mohamed, H.M.H. Abd El Bary, Decolorization of Mordant red 73 azo dye in water using $H_2O_2$/UV and photo-Fenton treatment, J. Hazard Mater. 174 (2010) 352–358.
[27] E. Yamal-Turbay, E. Jaén, M. Graells, M. Pérez-Moya, Enhanced photo-Fenton process for tetracycline degradation using efficient hydrogen peroxide dosage, J. Photochem. Photobiol. A 267 (2013) 11–16.
[28] A.C. Affam, M. Chaudhuri, S.M. Kutty, K. Muda, UV Fenton and sequencing batch reactor treatment of chlorpyrifos, cypermethrin and chlorothalonil pesticide wastewater, Int. Biodeterior. Biodegrad. 93 (2014) 195–201.
[29] J. Saien, V. Moradi, A.-R. Soleymani, Investigation of a jet mixing photo-reactor device for rapid dye discoloration and aromatic degradation via UV/$H_2O_2$ process, Chem. Eng. J. 183 (2012) 135–140.
[30] E. Cokay Catalkaya, F. Kargi, Advanced oxidation treatment of pulp mill effluent for TOC and toxicity removals, J. Environ. Manag. 87 (2008) 396–404.
[31] A. Karcia, I. Arslan-Alatonb, T. Olmez-Hanci, M. Bekbölet, Transformation of 2, 4-dichlorophenol by $H_2O_2$/UV-C, Fenton and photo-Fenton processes: oxidation products and toxicity evolution, J. Photochem. Photobiol. A 230 (2012) 65–73.
[32] H.M. Kim, J.G. Kim, J.D. Cho, J.W. Hong, Optimization and characterization of UV curable adhesives for optical communication by response surface methodology, Polym. Test. 22 (2003) 899–906.
[33] J.P. Wang, Y.Z. Chen, X.W. Ge, H.Q. Yu, Optimization of coagulation- flocculation process for a paper-recycling wastewater treatment using response surface methodology, Colloids Surf. A: Physicochem. Eng. Asp. 302 (2007) 204–210.
[34] O.B. Ayodele, J.K. Lim, B.H. Hameed, Degradation of phenol in photo-Fenton process by phosphoric acid modified kaolin supported ferric-oxalate catalyst: optimization and kinetic modeling, Chem. Eng. J. 197 (2012) 181–192.
[35] Z.M. Shaykhi, A.A.L. Zinatizadeh, Statistical modeling of photocatalytic degradation of synthetic amoxicillin wastewater (SAW) in an immobilized $TiO_2$ photocatalytic reactor using response surface methodology (RSM), J. Taiwan Inst. Chem. Eng. 45 (2014) 1717–1726.
[36] A. Suárez-Escobar, A. Pataquiva-Mateus, A. López-Vasquez, Electrocoagulation—photocatalytic process for the treatment of lithographic wastewater. Optimization using response surface methodology (RSM) and kinetic study, Catal. Today 266 (2016) 120–125.
[37] R.H. Myers, D.C. Montgomery, Response Surface Methodology: Process and Product Optimization using Designed Experiments, 2nd ed., John Wiley & Sons, USA, 2002.
[38] N. Aslan, Application of response surface methodology and central composite rotatable design for modeling and optimization of a multi-gravity separator for

chromite concentration, Powder Technol. 185 (2008) 80–86.
[39] M.J. Anderson, P.J. Whitcomb, RSM Simplified: Optimizing Processes Using Response Surface Methods for Design of Experiments, Productivity Press, New York, 2005.
[40] M.A. Alim, J.H. Lee, C.C. Akoh, M.S. Choi, M.S. Jeon, J.A. Shin, K.T. Lee, Enzymatic transesterification of fractionated rice bran oil with conjugated linoleic acid: optimization by response surface methodology, LWT-Food Sci. Technol. 41 (2008) 764–770.
[41] R.H. Myers, D.C. Montgomery, C.M. Anderson-Cook, Response Surface Methodology: Process and Product Optimization Using Designed Experiments, third ed., John Wiley Inc, New Jersey, 2009.
[42] T.U. Nwabueze, Basic steps in adapting response surface methodology as mathematical modelling for bioprocess optimization in the food systems, Int. J. Food Sci. Technol. 45 (2010) 1768–1776.
[43] M. Demirel, B. Kayan, Application of response surface methodology and central composite design for the optimization of textile dye degradation by wet air oxidation, Int. J. Ind. Chem. 3 (2012) 24.
[44] B. Tak, B.S. Tak, Y. Kim, Y. Park, Y. Yoon, G. Min, Optimization of color and COD removal from livestock wastewater by electrocoagulation process: application of Box–Behnken design (BBD), J. Ind. Eng. Chem. 28 (2015) 307–315.
[45] H.Y. Li, R. Priambodo, Y. Wang, H. Zhang, Y.H. Huang, Mineralization of bisphenol A by photo-Fenton-like process using a waste iron oxide catalyst in a three-phase fluidized bed reactor, J. Taiwan Inst. Chem. Eng. 53 (2015) 68–73.
[46] H.C. Lan, A.M. Wang, R.P. Liu, H.J. Liu, J.H. Qua, Heterogeneous photo-Fenton degradation of acid red B over $Fe_2O_3$ supported on activated carbon fiber, J. Hazard. Mater. 285 (2015) 167–172.
[47] U. Bali, U. Atalkaya, S. Fusun, Photodegradation of Reactive Black 5, Direct Red 28 and Direct Yellow 12 using UV, UV/$H_2O_2$ and UV/$H_2O_2$/$Fe^{2+}$: a comparative study, J. Hazard. Mater. B114 (2004) 159–166.
[48] R. Andreozzi, V. Caprio, A. Insola, R. Marotta, Advanced oxidation processes (AOP) for water purification and recovery, Catal. Today 53 (1999) 51–59.
[49] M. Kallel, C. Belaida, R. Boussahel, M. Ksibi, A. Montiel, B. Elleuch, Olive mill wastewater degradation by Fenton oxidation with zero-valent iron and hydrogen peroxide, J. Hazard. Mater. 163 (2009) 550–554.
[50] I. Carra, C. Sirtori, L. Ponce-Robles, J. Antonio Sánchez Pérez, S. Malato, A. Agüera, Degradation and monitoring of acetamiprid, thiabendazole and their transformation products in an agro-food industry effluent during solar photo-Fenton treatment in a raceway pond reactor, Chemosphere 130 (2015) 73–81.
[51] O. Primo, M.J. Rivero, I. Ortiz, Photo-Fenton process as an efficient alternative to the treatment of landfill leachates, J. Hazard. Mater. 153 (2008) 834–842.
[52] H. Mohan, J.P. Mittal, Formation and reactivity of the radical-cation of bromobenzene in aqueous-solution—a pulse-radiolysis study, J. Phys. Chem. 99 (1995) 6519–6524.
[53] C.L. Hsueh, Y.H. Huang, C.C. Wang, C.Y. Chen, Degradation of azo dyes using low iron concentration of Fenton and Fenton-like system, Chemosphere 58 (2005) 1409–1414.
[54] N. Modirshahla, M.A. Behnajady, F. Ghanbary, Decolorization and mineralization of C.I. Acid Yellow 23by Fenton and photo-Fenton processes, Dyes Pigm. 73 (2007) 305–310.
[55] R. Nageswara Rao, N. Venkateswarlu, The photocatalytic degradation of amino and nitro substituted stilbenesulfonic acids by $TiO_2$/UV and $Fe^{2+}$/$H_2O_2$/UV under aqueous conditions, Dyes Pigm. 77 (2008) 590–597.
[56] N. Daneshvar, M. Rabbani, N. Modirshahla, M.A. Behnajady, Photooxidative degradation of Acid Red 27 in a tubular continuous-flow photoreactor: influence of operational parameters and mineralization products, J. Hazard. Mater. 118 (2005) 155–160.
[57] S. Malato, P. Fernández-Ibánez, M.I. Maldonado, J. Blanco, W. Gernjak, Decontamination and disinfection of water by solar photocatalysis: recent overview and trends, Catal. Today 147 (2009) 1–59.
[58] I. Arslan-Alaton, N. Ayten, T. Olmez-Hanci, Photo-Fenton-like treatment of the commercially important H-acid: process optimization by factorial design and effects of photocatalytic treatment on activated sludge inhibition, Appl. Catal. B 96 (2010) 208–217.
[59] I.A. Alaton, S. Teksoy, Acid dyebath effluent pretreatment using Fenton's reagent: process optimization, reaction kinetics and effects on acute toxicity, Dyes Pigm. 73 (2007) 31–39.
[60] A. Rubio-Clemente, E. Chica, G.A. Peñuela, PetrochemicaL Wastewater Treatment by Photo-fenton Process, Water Air Soil Pollut. 226 (2015) 62–70.
[61] K. Thirugnanasambandham, V. Sivakumar, J. Prakash Maran, Response surface modelling and optimization of treatment of meat industry wastewater using electrochemical treatment method, J. Taiwan Inst. Chem. Eng. 46 (2015) 160–167.